Journal of South American Earth Sciences 104 (2020) 102853

Contents lists available at ScienceDirect

Journal of South American Earth Sciences

journal homepage: www.elsevier.com/locate/jsames

Eocene volcanism in the Fuegian Andes: Evidence from petrography and detrital zircons in marine volcaniclastic sandstones

Eduardo B. Olivero [a,b,*], Pablo J. Torres Carbonell [a], Martin Svojtka [c], Mark Fanning [d], Francisco Hervé [e,f], Daniel Nývlt [g]

[a] Centro Austral de Investigaciones Científicas (CADIC-CONICET), Bernardo Houssay 200, 9410, Ushuaia, Argentina
[b] Instituto de Ciencias Polares, Ambiente y Recursos Naturales (ICPA-UNTDF), Fuegia Basket 251, 9410, Ushuaia, Argentina
[c] Institute of Geology of the Czech Academy of Sciences, Rozvojová 269, 165 00, Praha 6, Czech Republic
[d] Research School of Earth Sciences, Australian National University, Canberra, ACT, Australia
[e] Universidad Andres Bello, Carrera de Geología, Santiago, Chile
[f] Universidad de Chile, Departamento de Geología, Santiago, Chile
[g] Czech Geological Survey, Klárov 3, 118 21, Praha 1, Czech Republic

ARTICLE INFO

Keywords:
FuegianAndes
Eocene volcanism
Detrital zircons
U–Pb dating
Austral-Magallanes basin

ABSTRACT

The sedimentology, petrography, and U–Pb dating of two Eocene volcaniclastic horizons of the Punta Torcida and Leticia formations, Austral basin, Tierra del Fuego, Argentina are interpreted and documented. The volcaniclastic deposits, pumicite breccia and tuffaceous sandstones, are formed by glass shards, plagioclase crystals, and pumiceous and lithic andesitic fragments. Originally deposited as tephra fallout, they have been subsequently reworked and redeposited in marine settings. The final deposits, however, are interpreted essentially as syn-eruptive. U–Pb dating of detrital zircons gave a 46.3 ± 0.4 Ma (early Lutetian) age for the top of the Punta Torcida Formation and 41.9 ± 0.71 (late Lutetian) to 39.6 ± 0.82 (Bartonian) ages for the Leticia Formation. Paleogene volcanic rocks are unknown in the Southern Patagonian-Fuegian Andes; hence the studied volcanic deposits with minimal reworking are important to evaluate the time lag between eruption and true depositional ages in detrital zircons. The resulting dates allow evaluating the timing of the important, basin-wide, intra-Eocene unconformity known from Tierra del Fuego to Lago Argentino, Santa Cruz, Argentina. The documented eruptive phases are related to Andean magmatism, probably located in the outcrop area of the Seno Año Nuevo suite in the Chilean Archipelago.

1. Introduction

Exposures of Paleogene volcanic rocks are unknown along the ~1000 km axial length of the Southern Patagonian-Fuegian Andes stretching from Lago Argentino (~50°S) to the easternmost Beagle Channel (~55°S) (Fig. 1). Late Cretaceous and Paleogene igneous rocks are only known from exposed plutons in the Chilean coastal archipelago and the main island of Tierra del Fuego (Hervé et al., 2007; González Guillot, 2016; Poblete et al., 2016), but their corresponding volcanic carapaces were probably eroded. Hence, time and spatial distribution of Paleogene volcanic activity is only indirectly recognized and mostly inferred from sedimentary petrography, detrital zircon data or from sediment source-to-sink pathways (e.g. Barbeau et al., 2009; McAtamney et al., 2011; Fosdick et al., 2015; Schwartz et al., 2017; Malkowski et al., 2017; George et al., 2020).

Large analytical data derived mainly from sedimentary petrography, including 150 studied thin-sections from ~4 km-thick Late Cretaceous to Oligocene marine successions from the thrust-fold belt of the Fuegian Andes resulted in the finding of two main sandstone detrital modes: a volcaniclastic, plagioclase-rich andesitic mode and a quartz-lithic mode (Olivero, 2002; Torres Carbonell and Olivero, 2019; Barbeau et al., 2009). Though there are some stratigraphic overlaps, at the large scale the volcaniclastic mode dominates the Upper Cretaceous-lower Eocene succession and the quartz-lithic mode dominates the late mid Eocene-Oligocene succession. The later succession rests on a regional, basin-wide unconformity (Fig. 2) recognized in the Austral-Magallanes basin from Tierra del Fuego (Olivero and Malumián, 1999, 2008; Torres Carbonell and Olivero, 2012; 2019, and bibliography therein) to

* Corresponding author. Centro Austral de Investigaciones Científicas (CADIC-CONICET), Bernardo Houssay 200, 9410, Ushuaia, Argentina.
E-mail address: emolivero@gmail.com (E.B. Olivero).

https://doi.org/10.1016/j.jsames.2020.102853
Received 14 July 2020; Accepted 27 August 2020
Available online 6 September 2020

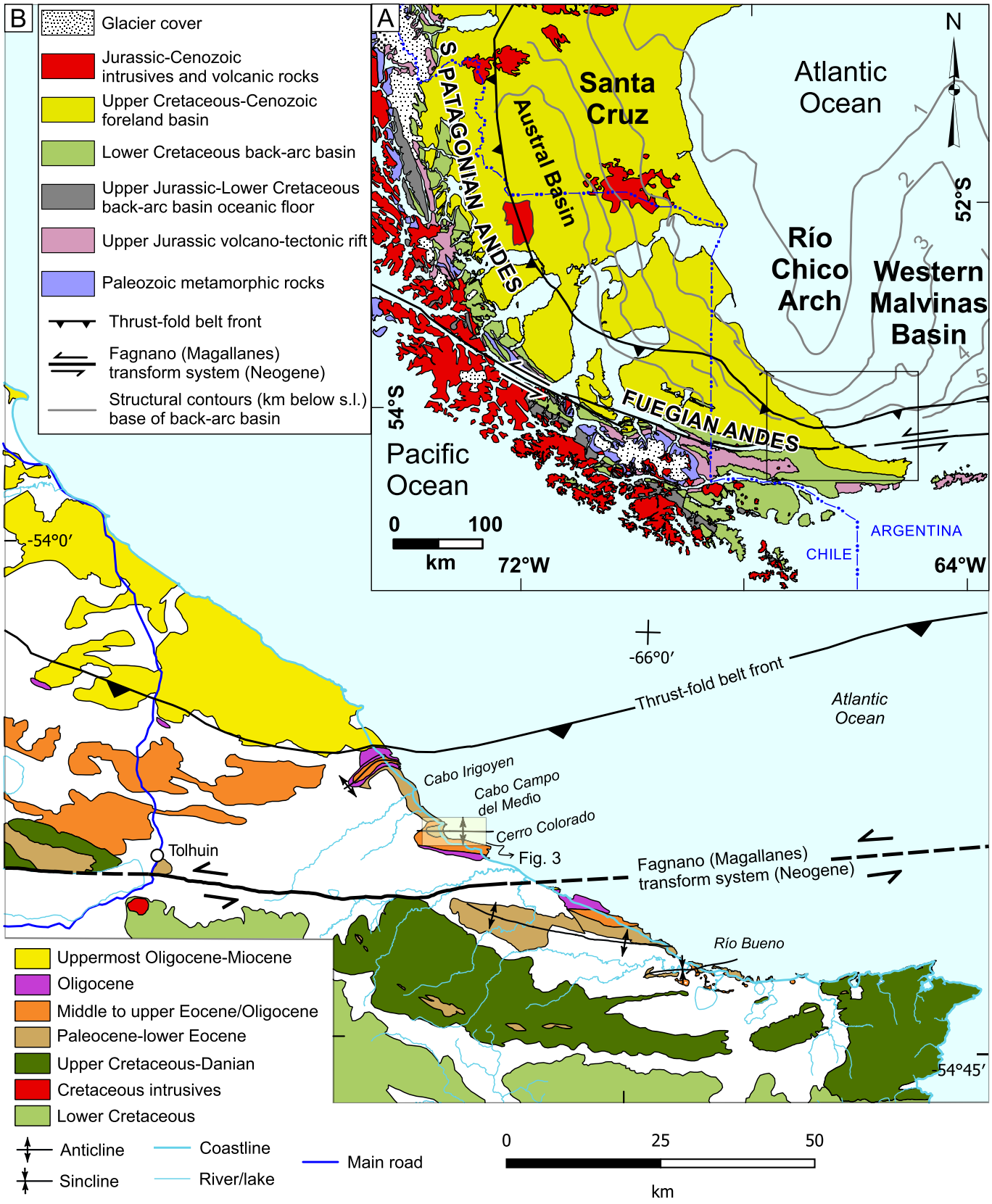

Fig. 1. Regional geological map of the Austral and Malvinas basins (A) and geological map of Tierra del Fuego (B) showing the location of Fig. 3, the study area at Cabo Campo del Medio Anticline. Modified from various sources (cf. Torres Carbonell and Olivero, 2019).

Lago Argentino (Malumián, 2002).

The timing and causes of formation of this basin-wide intra-Eocene unconformity are not well known. Within the fold-thrust belt of Tierra del Fuego this unconformity is remarkably well exposed in the study area, where it separates early Eocene to early mid Eocene turbidites of the Punta Torcida Formation from shallow-marine late mid Eocene sandstones of the Leticia Formation, with an estimated minimum hiatus of ~3 Myr (Olivero and Malumián, 1999; Torres Carbonell and Olivero, 2012; 2019). In the northwestern part of the Magallanes/Austral basin, however, the hiatus is considerably larger spanning up to ~20 Myr between the Maastrichtian/Danian Dorotea Formation and the mid Eocene Man Aike Formation (Malumián, 2002; Otero et al., 2013; Fosdick et al., 2015; George et al., 2020). It is not clear, however, if this large ~20 Myr hiatus includes erosional removal of a thick pile of previous late Paleocene-early Eocene deposits (e.g. Fosdick et al., 2015) –implying a significantly shorter non-depositional hiatus– or just non-deposition of this sedimentary pile during elaboration of the unconformity (e.g. George et al., 2020).

U–Pb ages obtained from volcanogenic detrital zircons are maximum depositional ages and the time difference with true depositional ages would depend on the duration of the time lag between phenocryst crystallization, extrusion, and final deposition. This lag is minimal for direct volcanic input, e.g. in tephra fallout deposits, but the time difference between volcanic events and true depositional ages may increase significantly with episodes of erosional removal and redeposition of detrital zircons. Hence, fresh volcanic materials or volcanic deposits with minimal reworking are extremely important to evaluate the time lag between volcanic activity and true depositional ages in detrital zircons (cf. Barbeau et al., 2009; Schwartz et al., 2017).

The main aim of this study is to document and date two thick Eocene volcaniclastic packages interpreted as the deposits of essentially synsedimentary volcanic activity. The older volcaniclastic package is located

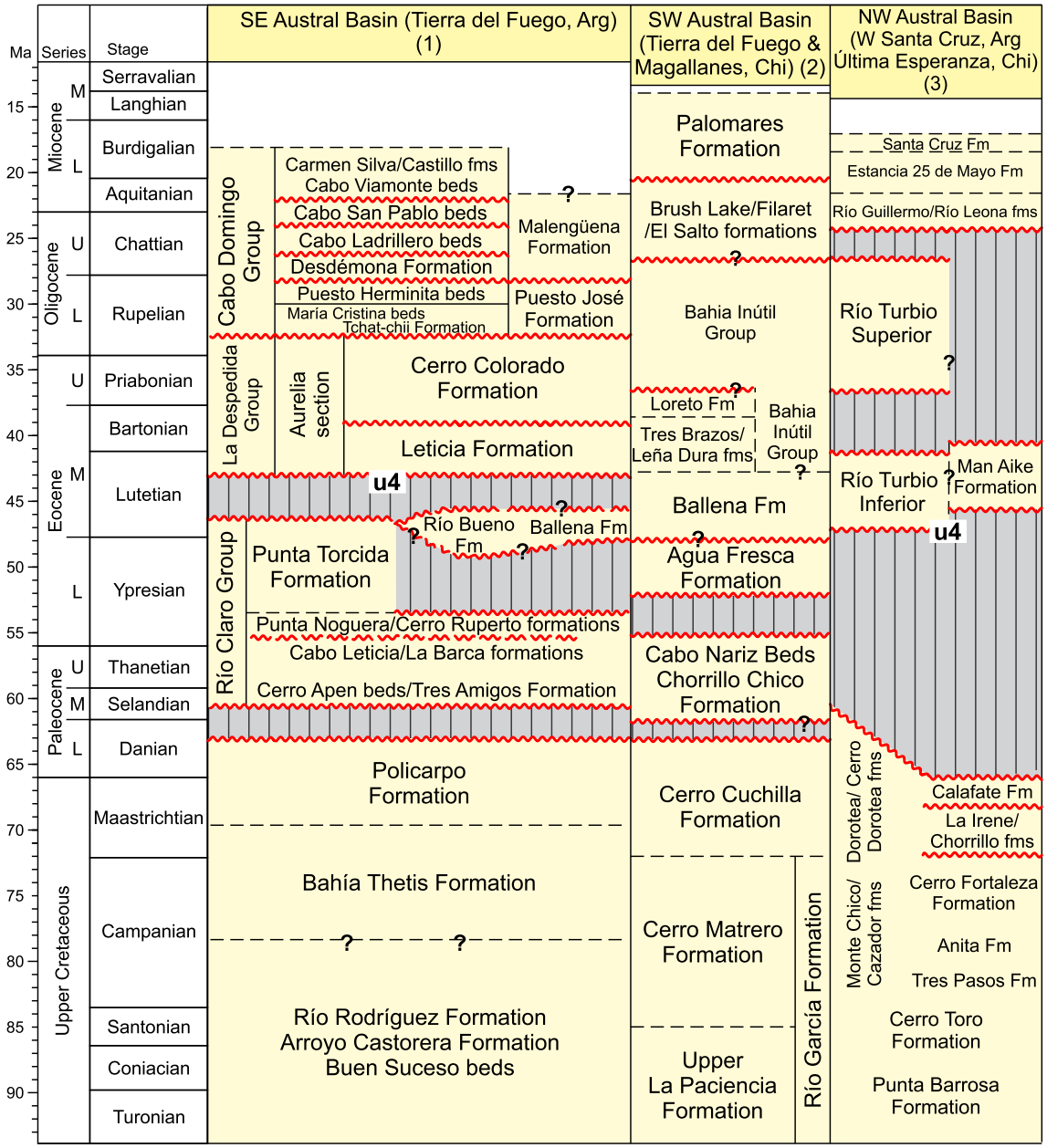

Fig. 2. Stratigraphic chart of the Austral-Magallanes basin Late Cretaceous-Cenozoic deposits in Tierra del Fuego and Patagonia, Argentina and Chile. Stratigraphy after: 1) Bedoya Agudelo (2019), Malumián and Olivero (2006), Martinioni (2010), Olivero and Malumián (2008), Torres Carbonell et al. (2009); 2) Biddle et al. (1986); McAtamney et al. (2011); Malumián et al. (2013); Fosdick et al. (2019); 3) Cuitiño et al. (2012), Fosdick et al. (2015), George et al. (2020), Malumián (2002).

on top of the early to early mid Eocene turbidites of the Punta Torcida Formation, just underneath the regional intra-Eocene unconformity. The younger volcaniclastic package is located atop the late mid Eocene shallow marine sandstones of the Leticia Formation. These volcaniclastic packages offer considerable interest and we shall argue through the study that they represent: 1) Eocene volcaniclastic deposits with minimal reworking, so far the only known of such deposits in the thrust-fold belt of the Fuegian Andes and likely in the whole Austral- Magallanes basin; 2) they have a key role for the absolute age assignation of two separate, but close volcanic events; 3) they are important for proper evaluation of U–Pb maximum depositional ages from detrital zircon throughout the Eocene in the Austral-Magallanes basin; and 4) they offer the possibility to better constrain the hiatus involved in the development of the regional intra-Eocene unconformity in the Fuegian Andes.

2. Materials and methods

Two samples with detrital zircons, CM 282–5 from the Punta Torcida Formation and CM 25 from the Leticia Formation, were analyzed for LA ICP-MS and SHRIMP U–Pb geochronology. In sample CM 282–5 zircon grains were concentrated by conventional methods and analyzed using an Element 2 (Thermo Scientific) high-resolution sector field mass spectrometer coupled with a 213-nm NdYAG UP-213 excimer laser ablation system (New Wave Research), housed at the Institute of Geology of the Czech Academy of Sciences, Praha. The laser was fired at a repetition rate of 5 Hz, using a spot size of 25 μm and a fluence of c. 5–6 J/cm^2. Natural zircon reference material 9150091500 (1065 Ma, Wiedenbeck et al., 1995) and its measurement uncertainties were used as isotopic calibration primary standard for normalization of all unknowns,

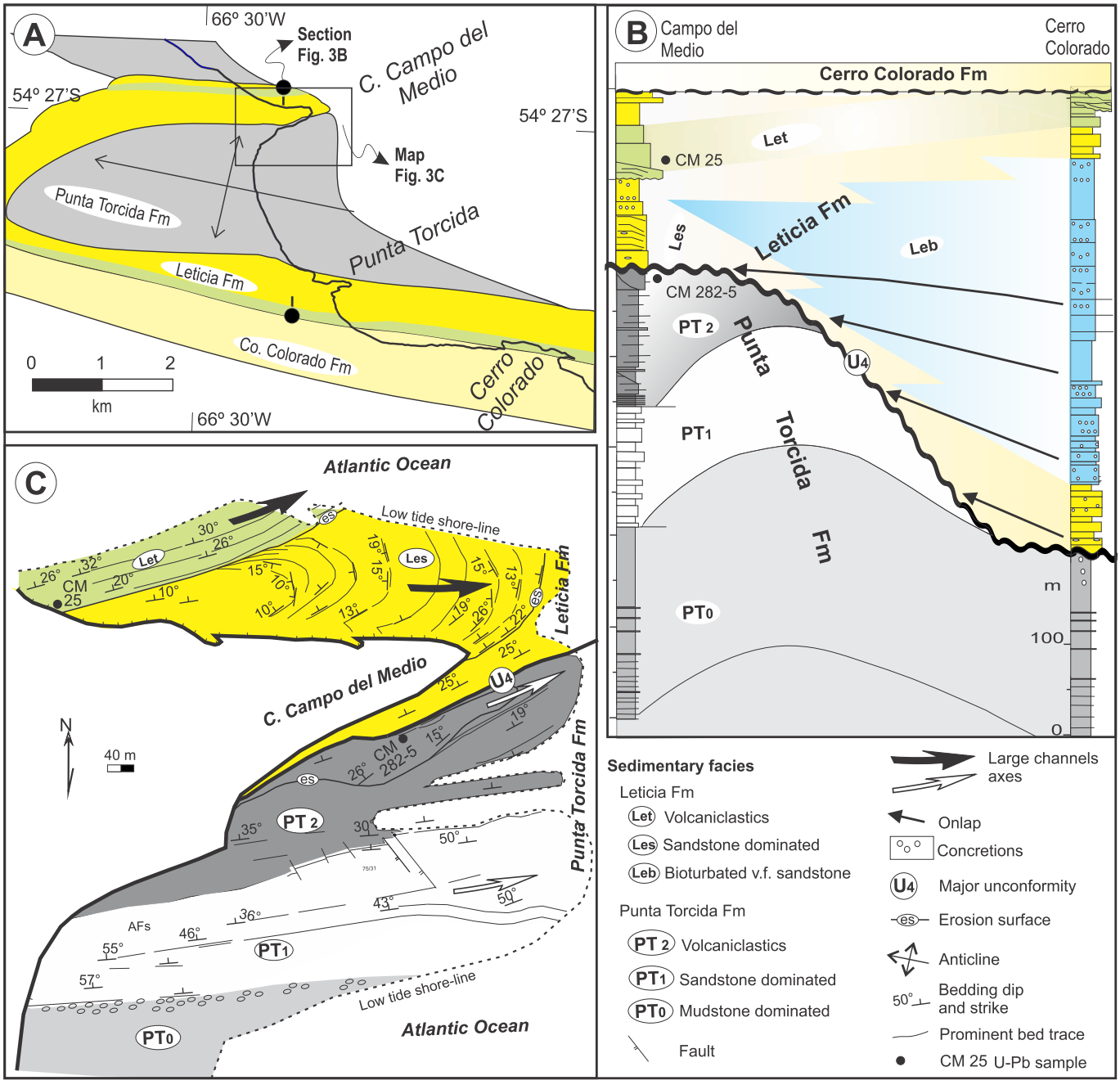

Fig. 3. Geology of the study area at Cabo Campo del Medio Anticline, see location in Fig. 1. Simplified geological map (A), stratigraphic section of the Punta Torcida and Leticia formations (B) and detailed map at Cabo Campo del Medio Anticline (C).

including validation zircon reference secondary material: GJ-1 (609 Ma, Jackson et al., 2004) that were periodically analyzed during the measurement for quality control. These values correspond well and are less than 1% accurate within the above published reference values (ESM Supp. DataTable 1). The U–Th–Pb isotopic ages shown in concordia diagrams (Fig. 5) were generated with Iolite (Paton et al., 2011) and Isoplot programs (v 3.75; Ludwig, 2012). U–Pb data are filtered to remove analyses that are >2% discordant.

In sample CM 25 zircon concentrates were prepared at the Departamento de Geología, Universidad de Chile. The U–Pb ages (Supp. Data Table 2) determined during this investigation were obtained using SHRIMPs I, II and RG at the Research School of Earth Sciences, the Australian National University, Canberra. The measurement techniques and data processing are those described by Williams (1998) as explained in Hervé et al. (2007).

The geographic coordinates of the samples are: CM 282–5, 54°27′06.23"S, 66°28′49.02"W; and CM 25, 54°27′01.05"S, 66°29′23.24"W.We use the Eocene time scale published in Gradstein et al. (2012).

3. Geological setting

The Austral-Magallanes is a large foreland basin system that extends along the front of the southernmost Andes, from northwestern Santa Cruz (Argentina) and eastern Magallanes-Última Esperanza (Chile) to the offshore extension of the system in the South Atlantic Ocean (Fig. 1), where it connects with the Western Malvinas basin (Biddle et al., 1986; Galeazzi, 1998; McAtamney et al., 2011; Sachse et al., 2015; Malkowski et al., 2017; Torres Carbonell and Olivero, 2019). In Tierra del Fuego, Argentina (Fig. 1), the Upper Cretaceous-Cenozoic sedimentary infill of the Austral-Magallanes basin accumulated synchronous with several contractional stages that followed a major ductile deformation phase, associated with the closure and inversion of the predecessor Late Jurassic-Early Cretaceous Rocas Verdes back-arc basin (Dalziel, 1981; Klepeis et al., 2010; Torres Carbonell et al., 2017, and the bibliography therein).

The progressive evolution of the Late Cretaceous-Cenozoic stratigraphy, depositional environments, and tectonic structures of the Austral-Malvinas foreland basin in Tierra del Fuego, Argentina, have been systematically studied during the last two decades by part of the present authors (EBO and PTC). A synthesis of this evolution can be found in Olivero et al. (2002, 2003); Malumián and Olivero (2006); Olivero and Malumián (1999, 2008); López Cabrera et al., (2008); Ponce (2009); Torres Carbonell (2010); Torres Carbonell et al., (2008, 2011; 2014; 2017); Martinioni (2010); Bedoya Agudelo (2019); Torres Carbonell and Olivero (2012, 2019) and bibliography therein. From the Late Cretaceous to the Oligocene-earliest Miocene, the sedimentary fill of the foreland basin system includes thick, unconformity-bounded, synteconic clastic wedges accumulated in successive elongated depocenters oriented subparallel to the Fuegian Andes. Sedimentation of these clastic wedges was closely related to the evolution of the Fuegian thrust-fold belt and dominated by axial and transverse turbidite systems, the clastic material of which was derived from the Fuegian Andes and the Fuegian-South Patagonian andesitic magmatic arc. South of the deformation front and within the thrust-fold belt, the turbidite systems include Campanian-Danian (Bahia Thetis and Policarpo formations); Paleocene-lower mid Eocene (Río Claro Group); upper mid Eocene-Oligocene (La Despedida Group); and part of Oligocene-Miocene (Cabo Domingo Group) deposits. North of the deformation front, the major part of the Cabo Domingo Group consists of subhorizontal strata (Fig. 1).

Our study is located along the Atlantic shore and south of the deformation front, in the Cabo Campo del Medio-Cerro Colorado area (Figs. 1 and 3). At this locality, the basin-wide intra Eocene unconformity is superbly exposed. This angular unconformity separates the early Eocene to basal mid Eocene Punta Torcida Formation of the Río Claro Group, from the late mid Eocene Leticia Formation of the La Despedida Group (Olivero and Malumián, 1999, 2008; Torres Carbonell et al., 2008; 2011). The intra Eocene unconformity marks a major change of sedimentary facies and sedimentary petrography, reflecting an important tectonic control on depositional environments. Beneath the unconformity, the Punta Torcida Formation consists of a deep-water turbidity system that filled and elongated foredeep, the evolution of which is intimately related to the northward propagation of the thrust-fold belt during the early Eocene-early mid Eocene (Torres Carbonell and Olivero, 2012, 2019). The sedimentary petrography of the Punta Torcida Formation, as well as that of the rest of Paleocene-Eocene deposits of the Río Claro Group, is dominated by volcaniclastic components derived from the Fuegian-South Patagonian andesitic arc (Olivero, 2002; Torres Carbonell and Olivero, 2019). Above the unconformity, the Leticia Formation is characterized by shallow-water settings (Olivero and Malumián, 1999, 2008; López Cabrera et al., 2008; Torres Carbonell and Olivero, 2012) and the sedimentary petrography is dominantly characterized by quartz-lithic components, mostly derived from older stratigraphic units of the Fuegian Andes and following a typical unroofing pattern (Olivero, 2002; Barbeau et al., 2009; Torres Carbonell and Olivero, 2019). These notable sedimentary changes in the Leticia Formation reflect a major orogenic exhumation of the southernmost Andes and deposition in a newly formed depocenter above the angular unconformity. This new depocenter was interpreted as a wedge-top depocenter denominated Maria Luisa sub-basin (Torres Carbonell et al., 2008, 2009).

4. Punta Torcida Formation

4.1. Sedimentary facies and petrography

At the type locality of Punta Torcida-Cabo Campo del Medio anticline, the Punta Torcida Formation has a minimum thickness of about 450 m and consists of a stacking of three major sedimentary packages, informally denominated PT_0, PT_1, and PT_2 (Fig. 3). The base of the Formation is not exposed; the top of the Formation is a marked angular unconformity with the Leticia Formation. At the southern limb of the Cabo Campo del Medio anticline, the PT_1 and PT_2 packages were eroded and the Leticia Formation unconformably covers the PT_0 package (Olivero and Malumián, 1999, 2008; Torres Carbonell and Olivero, 2012).

The lower mudstone-dominated sedimentary package PT_0, cropping out near the anticline axis is strongly deformed, making difficult to measure a continuous section. Nonetheless, partial sections including the informal members Pta, Ptb, and Ptc of Olivero and Malumián (1999) sum up a minimum of c. 200 m of thick mudstone beds and thin, fine-grained sandstone interbeds (Fig. 1). The informal members Pta-b-c are characterized by variable proportions of thin-bedded, fine-grained sandy turbidites, depicting Bouma Tb-c-d/e divisions, with common convolute bedding, climbing ripples, and thin horizons of slumped beds (Torres Carbonell and Olivero, 2012). The sandstone petrography (Olivero, 2002) is dominantly composed of volcaniclastic components, characterized by abundant andesitic fragments (Lv = 60–93%). Zonal plagioclase crystals are commonly abundant (P = 19–34%) and monocrystaline quartz grains are scarce (Qm = 7–10%).

The PT_1 package consists of thick intervals of interbedded fine-to very fine-grained tuffaceous sandstones and thinner intervals dominated by mudstones with interbedded sandstones. The facies association of the PT_1 package constitutes a turbidite system defining large channel-like lenticular geometries (Fig. 3) with variable thicknesses, ranging from 86 to 138 m (Torres Carbonell and Olivero, 2012). The sandstone-dominated intervals consist mostly of parallel laminated, fine-grained sandstone with abundant soft deformation structures and occasional intercalations of current ripple cross bedding. Less common are thinner beds of classical turbidites depicting Bouma Ta-e divisions and intercalated mudstones. Some fluted sandstone bases bear the graphoglyptid trace fossils *Helicolithus* isp., *Helicorhaphe* isp.,

Megagraptum submontanum, and *Paleodictyon majus*. In addition, several sandstones bear abundant structures of *Ophiomorpha rudis* and *Zoophycos* isp. (López Cabrera et al., 2008). The petrography of the PT_1 sandstone beds is similar to that of the PT_0 package.

The PT_2 package is up to 116 m thick and forms the upper part of the studied succession at Cabo Campo del Medio (Figs. 3 and 4; Torres Carbonell and Olivero, 2012; 2019). The PT_2 package is dominated by volcaniclastic breccia with alternations of sandy turbidites and minor lenticular mudstone and shell fragment interbeds. The dominant volcaniclastic breccias bear abundant angular pumicite fragments with the original volcanic glass still preserved in some fragments (e.g. Fig. 4F–H), but commonly the glass has been devitrified into a greenish, dense aggregate of small chlorite crystals (e.g. Fig. 4B, 4C, 4E). The base of some volcaniclastic breccias shows synsedimentary soft-deformation structures, characterized by ball and pillow structures (Fig. 4B). Most of the volcaniclastic breccias of the PT2 package are densely bioturbated, commonly with partial obliteration of bedding surfaces. Individual trace fossils are difficult to identify, but large traces of *Zoophycos* sp. are commonly discernible (López Cabrera et al., 2008).

The sandy turbidites, c. 50 cm thick, of the PT_2 package include two facies, one consists of structureless or roughly laminated, normally graded medium-grained sand intervals, with erosive bases and flute cast structures, covered by parallel laminated and ripple or climbing ripple-laminated intervals of fine-grained sandstone, usually with deformed ripple cross lamination at the top that grade to silty mudstone. The other sandy turbidite facies consists of fine-grained sandstones with profuse parallel lamination. The volcaniclastic breccias are interstratified with bioturbated, very fine-grained tuffaceous sandstones and mudstones bearing abundant shell fragments (Fig. 4C), dominated by the bivalve *Nucula* sp., with occasional scaphopods and gastropods.

Stratal geometry of the PT_2 package are characterized by lenticular bodies that commonly rest on scoured steep surfaces with variable dimensions, ranging from smaller lenses, c. 2 m wide, to larger channel-form bodies with widths of c. 50 m and more than 200 m in length (Fig. 3C; 4A). Paleocurrent vectors measured in flute casts and ripple cross-lamination are parallel to the axis of large channels and indicate a northeastward to eastward general paleoflow (Fig. 3C). The depositional paleoenvironments of the Punta Torcida Formation are interpreted as deposits of channeled turbidite systems, with channel or channel margin facies (PT_1-PT_2 packages) and probably overbank-levee or interchannel-basinal facies (PT_0 package) (Torres Carbonell and Olivero, 2012).

The petrography of the volcaniclastic breccias and turbidite sandstones of the PT_2 package (Olivero, 2002; Torres Carbonell and Olivero, 2019, Fig. 4F–H) is dominantly composed of volcaniclastic fragments, mostly pumicite and andesitic lithic fragments (Lv = 60–90%). Zonal, euhedral plagioclase (andesine) crystals are commonly abundant (P = 40-7%) and monocrystaline quartz grains are very scarce or absent (Qm = 0–3%). Pumicite volcanic glass is commonly devitrified to a greenish mass of chlorite and/or glauconite, the latter is sometimes very abundant making up to 30% of the total volcanic lithic fragments.

4.2. Detrital zircon U–Pb dating

Most of the studied zircons from sample CM 282–5 are clear and dominated by euhedral, both short- and long-prismatic crystals, with subordinate needle crystals. Most of them are 150–360 μm long. Using CL imaging (Fig. 4D), internal zircon growth structures revealed predominantly igneous oscillatory zoning together with sector zoning, characteristic of slowly grown zircons in igneous settings (Hanchar and Miller, 1993). Laser ablation ICP-MS measurements of 22 zircon grains in sample CM 282–5 yield a scatter of U–Pb concordant ages between 45 Ma and 47 Ma (Supp. Data Table 1) with a resulting single concordia age of ca. 46.3 ± 0.4 Ma (2 σ, early Lutetian; Fig. 5).

Previously, Barbeau et al. (2009, their sample CI-PT1) have determined a detrital zircon maximum depositional age of 47.32 ± 0.77 Ma for the Punta Torcida Formation. The sample was recovered from a medium-grained, moderately sorted, subrounded litharenite bed that occurs within a thick succession of dark gray mudstones north of Cabo Irigoyen in the Atlantic coast of Tierra del Fuego. Identification of the stratigraphic location of this horizon (sample CI-PT1) in our section is not straightforward but most likely it would be located within the PT_0 or PT_1 informal packages of the type section of the Punta Torcida Formation at Cabo Campo del Medio.

5. Leticia Formation

5.1. Sedimentary facies and petrography

At the type locality of the Cabo Campo del Medio Anticline, the Leticia Formation rest on a high-relief angular unconformity (Figs. 3 and 4A), known as the U4 unconformity (Torres Carbonell et al., 2011). The relationship between the basal beds of the Leticia Formation and the U4 unconformity is a marked onlap (Figs. 3B and 4A). The top of the Formation is a planar unconformity developed at the contact with the late mid Eocene interval of the Cerro Colorado Formation. The Leticia Formation displays variable thicknesses and sedimentary facies on each limb of the anticline (Fig. 3B). At the southern limb, the Formation is c. 520 m thick and consists of three main facies associations: a lower sandstone-dominated facies (Les); a middle very fine-grained totally bioturbated sandstone facies (Leb); and an upper volcaniclastic facies (Let). At the northern limb of the anticline, the Leticia Formation, with a minimum thickness of c. 200 m, consists mostly of the Les and Let facies associations.

The package including the lower sandstone-dominated facies (Les) is recognized on both southern (c. 80 m thick) and northern (c. 100 m thick) limbs of the anticline (Fig. 3B). The Les interval is dominated by thick, up to 2–3 m, fine massive fine-grained sandstone beds, with subordinated fine conglomerate lenses and normally graded fine-sandstone beds. This thick-bedded horizon is followed upwards by well-stratified, fine-grained, glauconite sandstones with parallel lamination, sometimes with dense concentrations of carbonaceous particles, current and wave-ripple cross-laminae, herringbone cross-stratification, and occasional large (1 m thick) dunes, with asymptotic cross-bedding. Some beds bear relatively abundant trace fossils, including the ichnogenera *Curvolithus, Diplocraterion*, *Euflabella*, *Gyrochorte*, *Macaronichnus*, *Ophiomorpha*, *Patagonichnus*, *Schaubcylindrichnus*, and *Tasselia* (López Cabrera et al., 2008; Olivero and López Cabrera, 2013). In the northern limb of the anticline, this lower sandstone-dominated package is characterized by large channels, up to 250–300 m wide (Figs. 3C and 6A). The thick Leb interval (c. 350 m) is restricted to the southern limb of the anticline (Fig. 3B) and consists mostly of very fine-grained glauconitic sandstones, with the original bedding obliterated by bioturbation, which is characterized by a dense mottling with few recognizable trace fossils (López Cabrera et al., 2008; Olivero and López Cabrera, 2013). The sandstone petrography of the Les and Leb intervals is dominated by quartz-lithic fragments, with significant percentages of metamorphic rock fragments (especially quartz-sericite foliated rocks) and sedimentary-metasedimentary lithic fragments, and scarce volcanic rock fragments. Thus, they show a marked compositional change with respect to the Punta Torcida Formation (Olivero, 2002; Torres Carbonell and Olivero, 2019).

The upper part of the Leticia Formation is dominated by volcaniclastic, coarse-grained sandstone and fine breccia (Let facies), which are continuous across the Cabo Campo del Medio Anticline reaching nearly 40–50 m in the south and 60 m in the north (Fig. 3B–C). Large channels sometimes nested in successive levels recording heterolithic bedding, epsilon cross-bedding, and through cross-bedding are typical for this interval (Fig. 6A–C). The sandstone petrography of the Let interval is very distinctive and dominated by zonal, euhedral plagioclase (andesine) phenocrysts and fresh, volcanic glass, both as pumicite and glass shard fragments (Fig. 6D-E).

Paleocurrent vectors measured in current ripples and dunes are

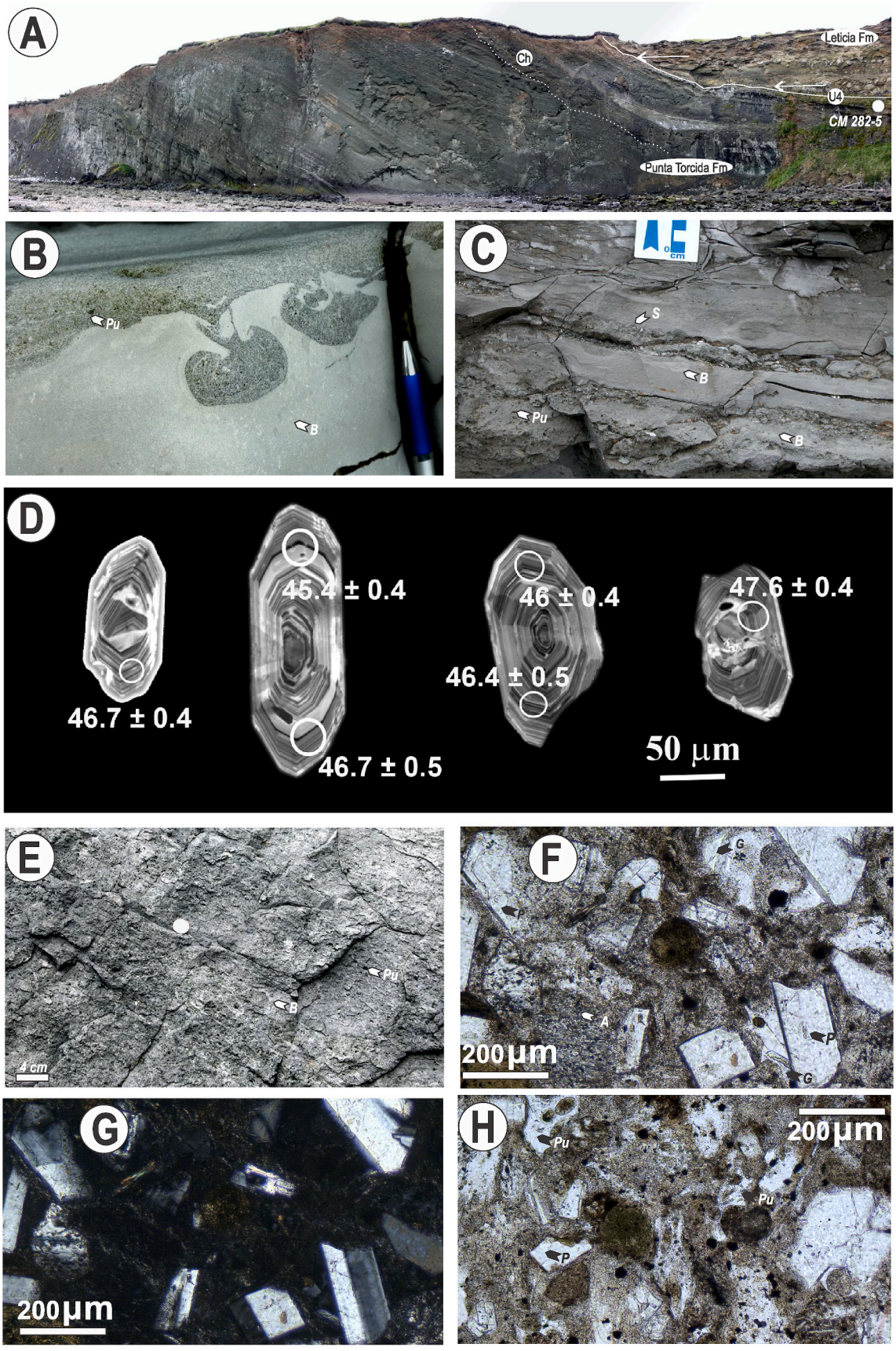

(caption on next page)

Fig. 4. Stratigraphy and petrography of the Punta Torcida Formation at Cabo Campo del Medio. **A**: Panoramic view of the channeled (Ch) PT_2 facies association of the Punta Torcida Formation, unconformably (U4) covered by the Leticia Formation. The horizon from which sample CM 282–5 was taken is shown. **B**: typical volcaniclastic facies of the PT_2; base of massive turbidite with ball and pillow soft deformation an abundant pumicite (Pu) fragments covering densely bioturbated (B) tuffaceous bed. **C**: alternating shell concentrations (S), bioturbated tuffaceous mudstones (B) and tuffaceous turbidites with abundant pumicites (Pu). **D**, **E**: bioturbated pumicite breccia of sample CM 282–5 (**E**), with zircon internal structures (CL image) showing U–Pb laser ablation ICP-MS analysis spots (25 μm) marked with concordant $^{206}Pb/^{238}U$ ages ± 2σ uncertainties (**D**). **F, G**: thin section of the pumicite horizon in Fig. 4C (**F**, plane-polarized light; **G**, cross-polarized light) showing abundant euhedral plagioclase crystals (P), glass shards (G), and andesitic fragments (A). **H**: thin section of sample CM 282–5, showing abundant euhedral plagioclase crystals (P) and pumicite fragments (Pu).

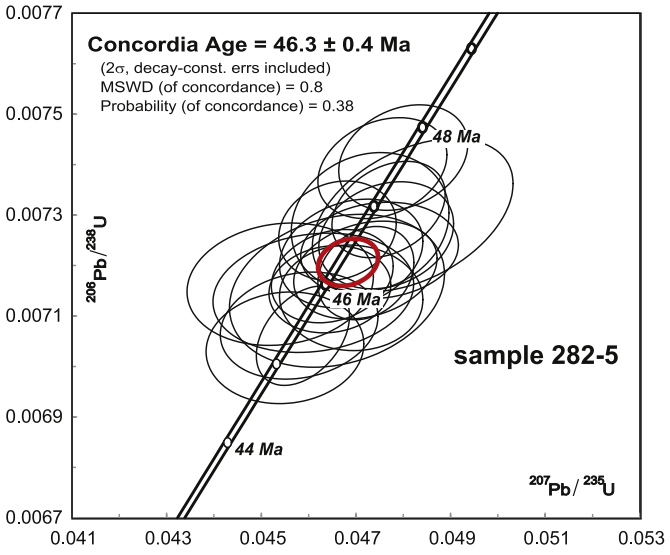

Fig. 5. U–Pb concordia diagram for sample CM 282–5 of the Punta Torcida Formation (22 analyses). All data are plotted with 2σ uncertainties.

directed to the east, which is coincident with the orientation of the main channel axes (Fig. 3C). Sedimentary facies and trace fossils of the Leticia Formation suggest shallow marine deposition, under partial influence of tides and waves (López Cabrera et al., 2008; Olivero and López Cabrera, 2013). Overall, it was interpreted as an aggradational-retrogradational-progradational succession filling a major erosive depression carved into the Punta Torcida Formation (Torres Carbonell and Olivero, 2019).

5.2. Detrital zircon U-Pb dating

The 95% of all detrital zircon grains (57 out of 60 grains) in sample CM 25 yields a range of U-Pb ages between 37 Ma and 48 Ma. The probability plot of the largest zircon grain population (95% of all grains) show three Eocene peaks: one in the Bartonian, 39.6 Ma; and two in the Lutetian, 41.9 Ma and 45.0 Ma (Fig. 7, right column). The 39.6 Ma and 41.9 Ma peaks are within the age range of calcareous nannoplankton and foraminifers of the Leticia Formation, which are interpreted as indicating the NP16 calcareous nannoplankton zone of Martini (1971), particularly the biostratigraphic range between c. 39–43 Ma within the NP16 zone (Olivero and Malumián, 1999; Malumián and Jannou, 2010; Bedoya Agudelo, 2019). Hence, the 39.6 and 41.9 Ma peaks are considered the closest ones to the depositional age of the Leticia Formation. The 45.0 Ma peak is closest to the age of the sample CM 282–5 (46.3 Ma) from the PT2 volcaniclastic facies of the Punta Torcida Formation. The rest of the zircon grains yield ages varying from 88.8 ± 1.5 Ma (Late Cretaceous, one grain); to 157 ± 2.3 Ma (Late Jurassic, one grain); and to 400.5 ± 5.3 Ma (Early Devonian, one grain) (Fig. 7; Supp. Data, Table 2).

6. Discussion

Large dataset of detrital zircon age spectra (e.g. Barbeau et al., 2009; McAtamney et al., 2011; Schwartz et al., 2017; Malkowski et al., 2017; Sickmann et al., 2019; Olivero et al., 2003, and references therein) combined with isotopic dating of igneous rocks and regional geologic studies (e.g. Dalziel, 1981; Suárez et al., 1985; Wilson, 1991; Biddle et al., 1986; Pankhurst et al., 2000; Fildani and Hessler, 2005; Hervé et al., 2007; Olivero and Malumián, 2008; Klepeis et al., 2010; González Guillot, 2016; Poblete et al., 2016; Torres Carbonell and Olivero, 2019) have provided important information on sediment source regions and provenance for most of the studied detrital zircons in the Late Cretaceous-Eocene sedimentary fill of the Austral-Magallanes basin in Southern Argentina and Chile.

Broadly defined, but with differences between regions along the ~1000 km axial length of the Southern Patagonian-Fuegian Andes, the main identified provenance of detrital zircons derived from Andean rocks includes: 1) mostly Paleozoic metasedimentary basement complexes; 2) Jurassic silicic to bimodal, rift-related volcanic rocks (Tobífera, Quemado, and Lemaire formations); and 3) Late Jurassic-Miocene Patagonian batholith (Barbeau et al., 2009; Schwartz et al., 2017; Malkowski et al., 2017; Sickmann et al., 2019). In the southernmost region, the Fuegian Andes are clearly differentiated from the northern Austral-Magallanes Andean regions because of: 1) dominance of arc-derived Late Cretaceous-Paleogene detrital zircons; 2) reduced presence of detrital zircons derived from Late Jurassic volcanic rocks for most of the Late Cretaceous-Early Eocene fill; and 3) very scarce detrital zircons derived from the Paleozoic basement (Barbeau et al., 2009; McAtamney et al., 2011).

The sandstone petrography of the Late Cretaceous-Miocene sedimentary fill of the Austral Magallanes basin in the Fuegian Andes presents also a very distinctive pattern (Olivero, 2002; Torres Carbonell and Olivero, 2019). The Qm-F-Lt and Qt-F-L modal sandstone petrography clearly discriminates Late Cretaceous-early mid Eocene from late mid Eocene-Miocene sedimentary successions. The older succession mainly includes the transitional and undissected magmatic-arc field of Dickinson et al. (1983), while the late mid Eocene-Miocene succession plot mainly in the recycled orogen field. Moreover, the lithic clasts composition shows a marked change from Late Cretaceous-early mid Eocene volcanic (andesitic)-rich mode to a late mid Eocene-Miocene metamorphic (quartz-sericite schists) and sedimentary-metasedimentary lithic–rich mode (Olivero, 2002; Torres Carbonell and Olivero, 2019). This notable shift in the sandstone modes is confirmed by a remarkable shift in the detrital zircon composition (Barbeau et al., 2009).

In the foreland strata of the Fuegian Andes, arc-derived detrital zircons were most likely sourced from magmatism in the Fuegian-South Patagonian Batholith, particularly from the mid-Late Cretaceous (126–74 Ma) Beagle suite, the Late Cretaceous rear-arc Fuegian Potassic Magmatism and Ushuaia Peninsula Andesites (84–68 Ma, González Guillot et al., 2018; Torres Carbonell et al., 2020) and the Paleogene (67–40 Ma) Seno Año Nuevo suite. Suárez et al. (1985) and Hervé et al. (2007) stressed the point that most granitoids of the Beagle and Seno Año Nuevo suites are represented by geographically restricted plutons, mostly emplaced in the far south. Hence, regional geologic distribution of Late Cretaceous-Paleogene granitoids (Suárez et al., 1985; Hervé et al., 2007; González Guillot, 2016) together with paleocurrent vectors of transverse and axial depositional systems (see Torres Carbonell and Olivero, 2019) and dominant detrital zircon composition (Barbeau et al., 2009; McAtamney et al., 2011), all offer consistent evidence for a dominant clastic procedence sourced from rocks exposed in the southern

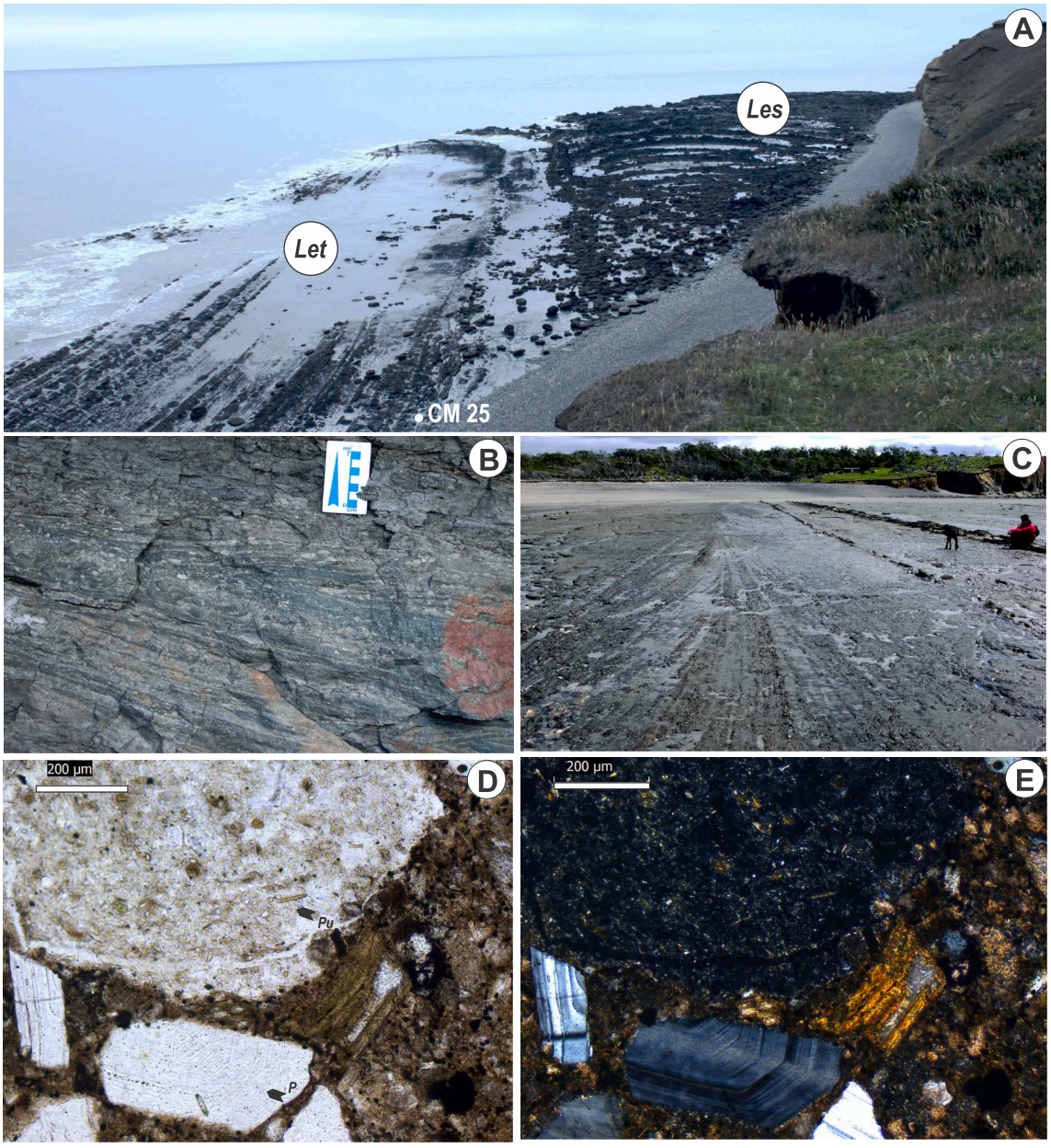

Fig. 6. Stratigraphy and petrography of the Leticia Formation at Cabo Campo del Medio. **A**: Large channels filled with volcaniclastic (Let) and sandstone-dominated (Les) sedimentary facies, see Fig. 3C for location and scale, depicting the stratigraphic horizon of sample CM 25. **B**: Cross-bedded tuffaceous breccia where sample CM 25 was collected. **C**: Channeled tuffaceous breccia with large epsilon cross-stratification, located between Punta Torcida-Cerro Colorado, same stratigraphic horizon with Let facies depicted in Fig. 5A–B. **D, E**: thin sections of sample CM 25 (**D**, plane-polarized light; **E**, cross-polarized light) showing abundant euhedral zoned plagioclase crystals (P) and pumicite fragments (Pu).

area.

No associated Late Cretaceous-Paleogene volcanic activity is known at present in the outcrop area of the Beagle suite, rear-arc, and Seno Año Nuevo suite granitoids (Hervé et al., 2007) or in the Fuegian Andes (Olivero and Malumián, 2008; González Guillot, 2016). However, the described thick horizons of volcaniclastic breccias and tuffaceous sandstones in the Punta Torcida (>100m-thick, PT_2) and Leticia (>50-60m-thick, Let) formations, point to the presence of at least two separate volcanic events. These volcaniclastic horizons are interpreted essentially as syn-eruptive deposits. They were not, however, directly originated from pyroclastic flows or tephra fallout deposition. Instead, the volcaniclastic materials show clear evidence of remobilization and redeposition in marine settings, such as displaced marine body fossils, abundant trace fossils, and channel-like geometries originated in deep-marine (Punta Torcida Formation; Fig. 4) or tidal (Leticia Formation; Fig. 6) settings. The composition of the volcaniclastic rocks of the PT_2 package in the Punta Torcida Fomation, or Let sedimentary facies in the Leticia Formations are exclusively or dominantly composed of pumicite, euhedral plagioclase crystals, and andesitic lithic fragments (Fig. 4F–H; 6D-E). On the contrary, epiclastic fragments are absent or very rare in these volcaniclastic facies. This suggests that the volcaniclastic material was mostly deposited on land from subaerial tephra fallout, during a relatively long period of time covering large areas and smoothing the landscape. Subsequently, fluvial erosion removed the volcaniclastic fragments delivering large volumes of pumice, glass shards, crystals, and lithic fragments to the sea, where they were distributed and redeposited in turbidite systems (PT_2) or tidal settings (Let).

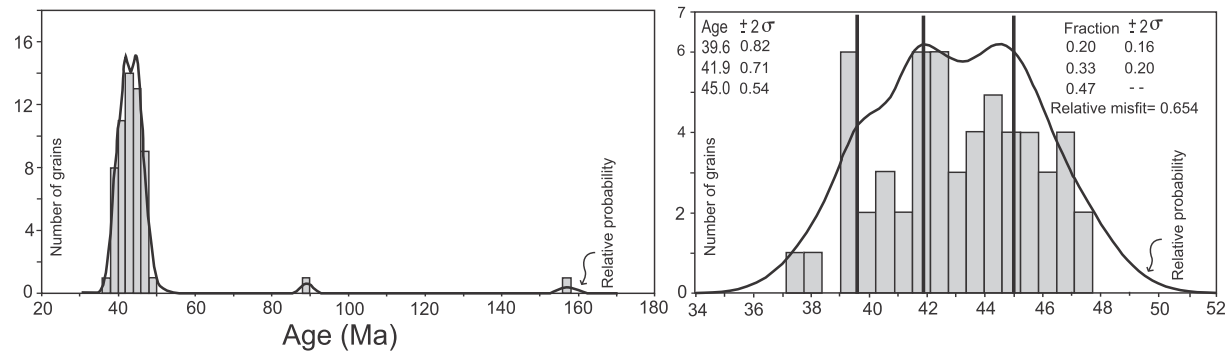

Fig. 7. Histogram and probability plot of detrital-zircon U-Pb age populations from sample CM 25, Leticia Formation. Left column depicts age distributions of all grains younger than 180 Ma (59 out of 60 grains). Right column depicts a close-up of the Paleogene portion of the probability distributions, including 57 out of 60 grains.

The envisaged scenario for deposition and remobilization of the volcaniclastic material is supported by the U–Pb age spectra in the analyzed detrital zircon grains of sample CM 25 from the Leticia Formation. In this sample, 95% of all detrital zircon grains cluster in three Eocene peaks of 39.6 Ma, 41.9 Ma, and 45.0 Ma (Fig. 7). The rest of the zircon grains (5%) are represented by three grains of Late Cretaceous; Late Jurassic, and Devonian age. This age distribution differs markedly from the histograms and probability plots of detrital zircon population analyzed from stratigraphically closer Eocene sedimentary samples in the Fuegian Andes (Barbeau et al., 2009). These analyses include zircon detrital grains from the Punta Torcida Formation and from members CCa and CCc of the Cerro Colorado Formation (Samples CI-PT; CCa1; and CCc1, respectively of Barbeau et al., 2009). All of them show age peaks of Late Cretaceous and/or Late Jurassic zircon grains and a large spread of age values, ranging from Paleogene to Paleozoic zircon grains (see Fig. 4 of Barbeau et al., 2009). Thus, the 95% cluster of Eocene zircon grains in sample CM 25 strongly supports the interpretation of essentially syn-eruptive remobilization and redeposition of the analyzed volcaniclastic horizon in the Leticia Formation.

The U–Pb age of the detrital zircons within the volcaniclastic horizon in the Punta Torcida Formation is clearly defined by the robust statistical value of 46.3 ± 0.4 Ma (Fig. 5), which is taken as the depositional age of the PT_2 package. The volcaniclastic horizon of the Leticia Formation includes two close U–Pb age values of 39.6 ± 0.82 Ma and 41.9 ± 0.71 Ma, which are consistent with the biostratigraphical reference to the NP16 calcareous nannoplankton zone (Malumián and Jannou, 2010; Bedoya Agudelo, 2019). Thus the depositional age of the Let horizon of the Leticia Formation is bracketed between 39.6 ± 0.82 Ma and 41.9 ± 0.71 Ma. The other Eocene peak of 45.0 ± 0.54 Ma is much older and probably corresponds to detrital zircons reworked from a previous eruptive phase of similar age than that of the volcaniclastic horizon in the Punta Torcida Formation. The maximum age difference between the top of the Punta Torcida Formation (sample CM 282–5, 46.3 ± 0.4 Ma) and the top of the Leticia Formation (Sample CM 25, 39.6 ± 0.82 Ma) is approximately 6.7 Myr considering the central peak ages, or 7.9 Ma considering the maximum and minimum 2 sigma uncertainities, respectively. However, the Leticia Formation is more than 500 m thick and thus, the hiatus involved in the U4 unconformity must be considerably less than 6 Myr. Based on biostratigraphy, the 500 m of the Leticia Formation are considered to represent no more than a 3 Myr duration (Malumián and Olivero, 2006), hence the hiatus involved in the U4 unconformity should encompass between c. 3.7–4.9 Myr.

As interpreted from the petrography, depositional settings, and U–Pb dating in detrital zircons, the depositional ages of the volcaniclastic PT2 package, Punta Torcida Formation, and the Let facies, Leticia Formation, are roughly coincident with syn-eruptive phases in the southern magmatic arc. The closest granitoid plutons of the Seno Año Nuevo suite, exposed in the Chilean Archipelago between Peninsula Hardy-Canal Ballenero, are located about 150–200 km to the SW of the present location of the studied area. They include Paleocene to Eocene diorite, tonalite and granodiorite plutons isotopically dated between 58.7 Ma and 40.3 Ma (Hervé et al., 2007; Poblete et al., 2016). As these records cover the span of the volcanic eruptive phases interpreted for the Punta Torcida (46.3 Ma) and Leticia (39.6 Ma and 41.9 Ma) formations, we think that the Seno Año Nuevo magmatism is a likely candidate for the source of the detected Eocene volcanism.

7. Conclusions

At the Cabo Campo del Medio Anticline area located on the Atlantic coast of Tierra del Fuego, Argentina (Figs. 1 and 3), two thick Eocene volcaniclastic packages almost exclusively composed of euhedral plagioclase crystals, glass shards, and pumicite and andesitic lithic fragments (Figs. 4 and 6) are interpreted as reworked syn-eruptive deposits. The older volcaniclastic package forms the uppermost stratigraphic levels of the Punta Torcida Formation (early Eocene-basal mid Eocene), which is part of a deep-marine, channeled turbidite system. The younger volcaniclastic package forms the uppermost stratigraphic levels of the Leticia Formation (late mid Eocene), characterized by shallow marine, partly tidal-influenced deposits.

U–Pb dating of detrital zircons recovered from two samples resulted in: a concordia age of 46.3 ± 0.4 Ma (early Lutetian) for the volcaniclastic package of the Punta Torcida Formation (Fig. 5); and three Eocene peaks of 39.6 ± 0.82 Ma, 41.9 ± 0.71 Ma, and 45.0 ± 0.54 Ma (Fig. 7) for the volcaniclastic package of Leticia Formation. The 39.6 Ma and the 41.9 Ma peaks are consistent with the NP16 calcareous nannoplankton zone assigned to the Leticia Formation, hence these peaks are interpreted to represent the depositional age of the Leticia Formation. The older peak of 45.0 Ma probably represents detrital zircons reworked from a previous eruptive phase of similar age than that of the volcaniclastic horizon in the Punta Torcida Formation.

The U–Pb age results indicate that the hiatus involved in the elaboration of the important basin-wide, intra-Eocene unconformity that separates the Punta Torcida and Leticia Formation in the study area spans no more than c. 3.7–4.9 Myr. This is a significantly shorter period than that of the c. 20 Myr, previously estimated at the northern part of the Austral Basin, in Última Esperanza, Chile, and Santa Cruz Province, Argentina.

Declaration of competing interest

The authors declare that they have no known competing financial interests or personal relationships that could have appeared to influence the work reported in this paper.

Acknowledgments

This study was supported by MEYS (Czech Republic) grant no. 7AMB12AR024 to MS and DN and institutional support RVO 67985831 to MS. Field work in Tierra del Fuego was supported by grant ARC/13/05 of the Program of Cooperation in Research and Development between MEYS (Czech Republic) and MINCYT (Argentina). Additional financing was obtained from ANPCyT-FONCyT PICT 2015 2982 and 0419, PUE CONICET 2016, and PIDUNTDF-A1.

Appendix A. Supplementary data

Supplementary data to this article can be found online at https://doi.org/10.1016/j.jsames.2020.102853.

References

Barbeau Jr., D.L., Olivero, E.B., Swanson-Hysell, N.L., Zahid, K.M., Murray, K.E., Gehrels, G.E., 2009. Detrital-zircon geochronology of the eastern Magallanes foreland basin: implications for Eocene kinematics of the northern Scotia Arc and Drake Passage. Earth Planet Sci. Lett. 284, 489–503.

Bedoya Agudelo, E.L., 2019. Asociaciones de nanofósiles calcáreos del Paleoceno-Mioceno de Tierra del Fuego. Bioestratigrafía, Paleoecología y Paleooceanografía. Tesis Doctoral, Facultad de Ciencias Exactas y Naturales. Universidad de Buenos Aire. Directores Drs. E.B. Olivero y A. Concheyro, Buenos Aires. http://digital.bl.fcen.uba.ar/Download/Tesis.

Biddle, K.T., Uliana, M.A., Mitchum Jr., R.M., Fitzgerald, M.G., Wright, R.C., 1986. The stratigraphy and structural evolution of the central and eastern Magallanes basin, southern South America. Foreland Basins. In: Allen, P.A., Homewood, P. (Eds.), 8. Special Publication of the International Association of Sedimentologists, pp. 41–66.

Cuitiño, J.I., Pimentel, M.M., Ventura Santos, R., Scasso, R.A., 2012. High resolution isotopic ages for the early Miocene "Patagoniense" transgression in Southwest Patagonia: stratigraphic implications. J. S. Am. Earth Sci. 38, 110–122. https://doi.org/10.1016/j.jsames.2012.06.008.

Dalziel, I.W.D., 1981. Back-arc extension in the southern Andes: a review and critical reappraisal. Philosophical Transactions of the Royal Society, London, Ser. A Mathematical and Physical Sciences 300 (1454), 319–335.

Dickinson, W.R., Beard, L., Brakenridge, G.R., Erjavec, J.L., Ferguson, R.C., Inman, K.F., Knepp, R.E.X.A., Lindberg, F., Ryberg, P.T., 1983. Provenance of North American Phanerozoic sandstones in relation to tectonic setting. Bull. Geol. Soc. Am. 94, 222–235.

Fildani, A., Hessler, A.M., 2005. Stratigraphic record across a retroarc basin inversion: Rocas Verdes–Magallanes basin, patagonian Andes, Chile. Geol. Soc. Am. Bull. 117, 1596–1614. https://doi.org/10.1130/B25708.1.

Fosdick, J.C., Grove, M., Graham, S.A., Hourigan, J.K., Lovera, O., Romans, B.W., 2015. Detrital thermochronologic record of burial heating and sediment recycling in the Magallanes foreland basin, Patagonia Andes. Basin Res. 27, 546–572. https://doi.org/10.1111/bre.12088.

Fosdick, J., VanderLeest, R., Bostelmann, E., Leonard, J., Ugalde, R., Oyarzún, J., Griffin, M., 2019. Revised Timing of Cenozoic Atlantic Incursions and Changing Hinterland Sediment Sources during Southern Patagonian Orogenesis. https://doi.org/10.31223/osf.io/vqkds. EarthArXiv [Preprint].

Galeazzi, J.S., 1998. Structural and stratigraphic evolution of the western Malvinas basin, Argentina. American Association of Petroleoum Geologists Bulletin 82, 596–636.

George, S.W.M., Davis, S.N., Fernández, R.A., Manríquez, L.M.E., Leppe, M.A., Horton, B. K., Clarke, J.A., 2020. Chronology of deposition and unconformity development across the cretaceous–paleogene boundary, Magallanes-Austral basin, patagonian Andes. J. S. Am. Earth Sci. 97 https://doi.org/10.1016/j.jsames.2019.102237.

González Guillot, M., 2016. Magmatic evolution of the southernmost Andes and its relation with subduction processes. In: Ghiglione, M.C. (Ed.), Geodynamic Evolution of the Southernmost Andes. Springer Earth System Sciences, Switzerland, pp. 37–74. https://doi.org/10.1007/978-3-319-39727-6_3.

González Guillot, M., Ghiglione, M., Escayola, M., Martins Pimentel, M., Mortensen, J., Acevedo, R., 2018. Ushuaia pluton: magma diversification, emplacement and relation with regional tectonics in the southernmost Andes. J. S. Am. Earth Sci. 88, 497–519. Journal of South American Earth Sciences 88, 497–519.

Gradstein, F.M., Ogg, J.G., Schmitz, M.D., Ogg, G.M. (Eds.), 2012. The Geologic Time Scale 2012, vols. 1–1. Elsevier Amsterdam, Boston, p. 144.

Hanchar, J.M., Miller, C.F., 1993. Zircon zonation patterns as revealed by cathodoluminescence and backscattered electron images: implications for interpretation of complex crustal histories. Chem. Geol. 110, 1–13.

Hervé, F., Pankhurst, R.J., Fanning, C.M., Calderón, M., Yaxley, G.M., 2007. The South Patagonian batholith: 150 my of granite magmatism on a plate margin. Lithos 97, 373–394. https://doi.org/10.1016/j.lithos.2007.01.007.

Jackson, S.E., Pearson, N.J., Griffin, W.L., Belousova, E.A., 2004. The application of laser ablation-inductively coupled plasma-mass spectrometry to in situ U–Pb zircon geochronology. Chem. Geol. 211, 47–69.

Klepeis, K.A., Betka, P., Clarke, G., Fanning, M., Hervé, F., Rojas, L., Mpodozis, C., Thomson, S., 2010. Continental underthrusting and obduction during the cretaceous closure of the Rocas Verdes rift basin, cordillera Darwin, patagonian Andes. Tectonics 29 (3), TC3014.

López Cabrera, M.I., Olivero, E.B., Carmona, N.B., Ponce, J.J., 2008. Cenozoic trace fossils of the cruziana, Zoophycos, and nereites ichnofacies from the fuegian Andes, Argentina. Ameghiniana 45, 377–392.

Ludwig, K.R., 2012. Isoplot V. 3.75—A Geochronological Toolkit for Microsoft Excel, vol. 5. Berkeley Geochronology Center, Special Publication, pp. 1–75.

Malkowski, M.A., Schwartz, T.M., Sharman, G.R., Sickmann, Z.T., Graham, S.A., 2017. Stratigraphic and provenance variations in the early evolution of the Magallanes-Austral foreland basin: implications for the role of longitudinal versus transverse sediment dispersal during arc-continent collision. Geol. Soc. Am. Bull. 129, 349–371. https://doi.org/10.1130/B31549.1.

Malumián, N., 2002. El terciario marino de la provincia de Santa Cruz. In: Haller, M.J. (Ed.), Geología y Recursos Naturales de Santa Cruz, Relatorio I, vol. 14, pp. 237–244.

Malumián, N., Olivero, E.B., 2006. El Grupo Cabo Domingo, Tierra del Fuego: bioestratigrafía, paleoambientes y acontecimientos del Eoceno-Mioceno marino. Rev. Asoc. Geol. Argent. 61, 139–160.

Malumián, N., Jannou, G., 2010. Los Andes Fueguinos: el registro micropaleontológico de los mayores acontecimientos paleooceanográfícos australes del Campaniano al Mioceno. Andean Geol. 37, 345–374.

Malumián, N., Hromic, T., Nañez, C., 2013. El Paleógeno de la cuenca de Magallanes: Bioestratigrafía y discontinuidades, vol. 4. Anales del Instituto de la Patagonia (Chile), pp. 29–52.

McAtamney, J., Klepeis, K., Mehrtens, C., Thomson, S., Betka, P., Rojas, L., Snyder, S., 2011. Along-strike variability of back-arc basin collapse and the initiation of sedimentation in the Magallanes foreland basin, southernmost Andes (53–54.5°S). Tectonics 30, TC5001. https://doi.org/10.1029/2010TC002826.

Martini, E., 1971. Standard Tertiary and Quaternary calcareous nannoplankton zonation. In: Farinacci, A. (Ed.), Proceedings of the II Planktonic Conference Roma, vol. 2. Edizioni Tecnoscienza, Rome, pp. 739–785.

Martinioni, D.R., 2010. Estratigrafía y sedimentología del Mesozoico Superior-Paleógeno de la Sierra de Beauvoir y adyacencias, Isla Grande de Tierra del Fuego, Argentina. Tesis Doctoral, Facultad de Ciencias Exactas y Naturales. Universidad de Buenos Aires, Buenos Aires. http://digital.bl.fcen.uba.ar/Download/Tesis/Tesis_4608_Martinioni.pdf.

Olivero, E.B., 2002. Petrografía sedimentaria de sistemas turbidíticos del Cretácico–Paleógeno, Andes Fueguinos: procedencia, volcanismo y deformación. Actas del 15° Congreso Geológico Argentino. Calafate, Santa Cruz, Argentina, pp. 611–612.

Olivero, E.B., Malumián, N., 1999. Eocene stratigraphy of southeastern Tierra del Fuego Island, Argentina. American Association of Petroleum Geology Bulletin 83, 295–313.

Olivero, E.B., Malumián, N., Palamarczuk, S., 2003. Estratigrafía del Cretácico Superior-Paleoceno del área de bahía Thetis, Andes Fueguinos, Argentina: acontecimientos tectónicos y paleobiológicos. Rev. Geol. Chile 30, 245–263.

Olivero, E.B., Malumián, N., Palamarczuk, S., Scasso, R.A., 2002. El Cretácico superior-Paleógeno del área del Río Bueno, costa atlántica de la Isla Grande de Tierra del Fuego. Rev. Asoc. Geol. Argent. 57, 199–218.

Olivero, E.B., Malumián, N., 2008. Mesozoic-cenozoic stratigraphy of the fuegian Andes, Argentina. Geol. Acta 6, 5–18.

Olivero, E.B., López Cabrera, M.I., 2013. *Euflabella* n. igen.: complex horizontal spreite burrows in Upper Cretaceous–Paleogene shallow-marine sandstones of Antarctica and Tierra del Fuego. J. Paleontol. 87, 413–426.

Otero, R.A., Oyarzún, J.L., Soto-Acuña, S., Yury-Yáñez, R., Gutiérrez, N., Le Roux, J., Torres, T., Hervé, F., 2013. Neoselachians and chimaeriformes (chondrichthyes) from the upper cretaceous–paleogene of sierra baguales, southernmost Chile. Chronostratigraphic, paleobiogeographic and paleoenvironmental implications. J. S. Am. Earth Sci. 48, 13–30.

Paton, C., Hellstrom, J., Paul, B., Woodhead, J., Hergt, J., 2011. Iolite: freeware for the visualisation and processing of mass spectrometric data. J. Anal. At. Spectrom. 26, 2508–2518.

Pankhurst, R.J., Riley, T.R., Fanning, C.M., Kelley, S.P., 2000. Episodic silicic volcanism in Patagonia and the antarctic Peninsula: chronology of magmatism associated with the break-up of gondwana. J. Petrol. 41, 605–625. https://doi.org/10.1093/petrology/41.5.605.

Poblete, F., Roperch, P., Arriagada, C., Ruffet, G., Ramirez de Arellano, C., Herve, F., Poujol, M., 2016. Late cretaceous – early Eocene counterclockwise rotation of the fuegian Andes and evolution of the patagonia-antarctic Peninsula system. Tectonophysics 668–669, 15–34. https://doi.org/10.1016/j.tecto.2015.11.025.

Ponce, J.J., 2009. Análisis estratigráfico secuencial del Cenozoico de la Cordillera Fueguina, Tierra del Fuego, Argentina. Doctoral thesis, unpublished. Departamento de Geologia Universidad Nacional del Sur, Bahía Blanca.

Sachse, V.F., Strozyk, F., Anka, Z., Rodriguez, J.F., di Primio, R., 2015. The tectonostratigraphic evolution of the Austral Basin and adjacent areas against the background of Andean tectonics, southern Argentina, South America. Basin Res. https://doi.org/10.1111/bre.12118.

Schwartz, T.M., Fosdick, J.C., Graham, S.A., 2017. Using detrital zircon U-Pb ages to calculate Late Cretaceous sedimentation rates in the Magallanes-Austral Basin, Patagonia. Basin Res. 29, 725–746. https://doi.org/10.1111/bre.12198.

Sickmann, Z.T., Schwartz, T.M., Malkowski, M.A., Dobbs, S.C., Graham, S.A., 2019. Interpreting large detrital geochronology data sets in retroarc foreland basins: an example from the Magallanes-Austral Basin, southernmost Patagonia. Lithosphere 11, 620–642. https://doi.org/10.1130/L1060.1.

Suárez, M., Hervé, F., Puig, A., 1985. Hoja Isla Hoste e islas adyacentes, XII Región. Carta Geológica de Chile 1:250.000, no. 65. Servicio Nacional de Geología y Minería, Chile, pp. 1–113.

Torres Carbonell, P.J., 2010. Control tectónico en la estratigrafía y sedimentología de secuencias sinorogénicas del Cretácico Superior-Paleógeno de la faja corrida y plegada Fueguina. Departamento de Geología, Universidad Nacional del Sur, Bahía Blanca. Doctoral thesis (unpublished).

Torres Carbonell, P.J., Olivero, E.B., Dimieri, L.V., 2008. Structure and evolution of the Fuegian Andes foreland thrust-fold belt, Tierra del Fuego, Argentina: paleogeographic implications. J. S. Am. Earth Sci. 25, 417–439. https://doi.org/10.1016/j.jsames.2007.12.002.

Torres Carbonell, P.J., Malumian, N., Olivero, E.B., 2009. El Paleoceno-Mioceno de Peninsula Mitre: antefosa y depocentro de techo de cuna de la cuenca Austral, Tierra del Fuego, Argentina. Andean Geol. 36, 197–235.

Torres Carbonell, P.J., Dimieri, L.V., Olivero, E.B., 2011. Progressive deformation of a Coulomb thrust wedge: the eastern Fuegian Andes thrust-fold belt. In: Poblet, J., Lisle, R. (Eds.), Kinematic Evolution and Structural Styles of Fold-And-Thrust Belts. Geological Society, London, Special Publications, Bath, pp. 123–147. https://doi.org/10.1144/SP349.7. The Geological Society.

Torres Carbonell, P.J., Olivero, E.B., 2012. Sand dispersal in the southeastern Austral Basin, Tierra del Fuego, Argentina: outcrop insights from Eocene channeled turbidite systems. J. S. Am. Earth Sci. 33, 80–101. https://doi.org/10.1016/j.jsames.2011.08.002.

Torres Carbonell, P.J., Dimieri, L.V., Olivero, E.B., Bohoyo, F., Galindo-Zaldivar, J., 2014. Structure and tectonic evolution of the Fuegian Andes (southernmost south America) in the framework of the scotia arc development. Global Planet. Change 123, 174–188. https://doi.org/10.1016/j.gloplacha.2014.07.019.

Torres Carbonell, P.J., Rodríguez Arias, L., Atencio, M.R., 2017. Geometry and kinematics of the Fuegian thrust-fold belt, southernmost Andes. Tectonics 36, 33–50.

Torres Carbonell, P.J., Olivero, E.B., 2019. Tectonic control on the evolution of depositional systems in a fossil, marine foreland basin: example from the SE Austral Basin, Tierra del Fuego, Argentina. Mar. Petrol. Geol. 104, 40–60. https://doi.org/10.1016/j.marpetgeo.2019.03.022.

Torres Carbonell, P.J., Cao, S.J., González Guillot, M., Mosqueira González, V.M., Dimieri, L.V., Duval, F., Scaillet, S., 2020. The Fuegian thrust-fold belt: from arc-continent collision to thrust-related deformation in the southernmost Andes. J. S. Am. Earth Sci. 102, 102678. https://doi.org/10.1016/j.jsames.2020.102678.

Wiedenbeck, M., Alle, P., Corfu, F., Griffin, W.L., Meier, M., Oberli, F., von Quadt, A., Roddick, J.C., Spiegel, W., 1995. Three natural zircon standards for U–Th–Pb, Lu–Hf, trace element and REE analyses. Geostand. Newsl. 19, 1–23.

Williams, I.S., 1998. U–Th–Pb geochronology by ion microprobe. In: McKibben, M.A., Shanks III, W.C., Ridley, W.I. (Eds.), Applications of Microanalytical Techniques to Understanding Mineralizing Processes, vol. 7. Reviews in Economic Geology, pp. 1–35.

Wilson, T.J., 1991. Transition from back-arc to foreland basin development in the southernmost Andes: stratigraphic record from the Ultima Esperanza District, Chile. Geol. Soc. Am. Bull. 103, 98–111. https://doi.org/10.1130/0016-7606, 1991.